

Texture Evolution in Low Carbon Steel Fabricated by Multi-directional Forging of the Martensite Starting Structure

Mehdi Salari^{1*}

¹Department of Metallurgy, Sirjan Branch, Islamic Azad University, Sirjan, 8915685718, Iran

*Email of Corresponding Author: mehsalari@gmail.com

Received: October 25, 2019; Accepted: February 20, 2020

Abstract

It has been clarified that deformation and annealing of martensite starting structure can produce ultrafine-grained structure in low carbon steel. This study aims to investigate the texture evolution and mechanical properties of samples with martensite structure deformed by two different forging processes. The martensitic steel samples were forged by plane strain compression and multi-directional forging up to the same true strain of 2. All samples were then annealed at 450 and 550°C for 30 min. It was found that the active slip systems in the BCC crystalline structure of martensite acted like ferrite steel. After the multi-directional forging of martensitic steel, the yield and ultimate strength greatly increased to 1278 and 1658 MPa, respectively. During annealing, in the plane strain compressed sample, the "oriented nucleation" and in the multi-directional forged specimen, the "selective growth" theory was dominant.

Keywords

Texture Evolution, Martensite Treatment, Multi-directional Forging, Plane Strain Compression, Low Carbon Steel

1. Introduction

Microstructures with ultra-fine grain sizes in bulk materials have gained popularity because of their outstanding mechanical properties such as high strength, high toughness, and super-plasticity at low temperatures [1].

Structural refinement by severe plastic deformation (SPD) is the most effective method for fabricating these advanced materials in bulk dimensions with a unique combination of properties.

Nowadays, the common SPD methods are equal-channel angular pressing (ECAP), accumulative roll bonding (ARB), equal channel angular extrusion/pressing (ECAE/ECAP), multi-directional forging (MDF) and high-pressure torsion (HPT), etc. Among the named techniques, the cheapest, simplest, and promising SPD technique is MDF [2].

Zheng et al. [3] applied the MDF to commercially pure titanium (CP Ti). They reported that with increasing the cycles of MDF, grain size and a fraction of low angle grain boundaries decreased.

Mikhaylovskaya et al. [4] investigated the microstructure evolution in the sample of an Al-Mg-Mn alloy during MDF. Expressive changes of mechanical properties and super-plasticity were detected due to the formation of a uniform fine grain structure 4.8 μm in size after MDF and consequent cold rolling.

Jiang et al. [5] examined the effect of changing cumulative strains on M50NiL steel during MDF. They reported that the mean grain size decreased to 1 μm at an aggregate strain of 7.2 and new small grains were nucleated at grain boundaries via dynamic recrystallization.

Kishchik et al. [6] studied the effect of MDF on the microstructure change of a conventional Al-Mg alloy in the strain range of 1.5 to 6.0, and in the temperature range of 200 to 500 $^{\circ}\text{C}$. They produced a homogeneous grain structure with an average grain size of 5 μm by SPD treatment, including MDF followed by 50% cold rolling and annealing at 450 $^{\circ}\text{C}$ for 30 min.

The other methods of producing ultra-fine grain structures consist of advanced thermo-mechanical processing, Such as martensite treatment that includes quenching, cold rolling of martensite and final annealing.

Hosseini et al. [7] clarified that rolling or plane strain compression (PSC) and annealing of martensite starting structure can produce nano/ultrafine-grained ferrite in low carbon steel. In their results, fully equiaxed grains, achieved from the martensite cell blocks during the annealing at 500 $^{\circ}\text{C}$ for sufficient time lengths.

Dastur et al. [8] concluded that an increase in nucleation sites through quenching and fragmentation of the obtained martensite laths during plastic deformation is the basis of grain refinement in the martensite treatment method. Yuan et al. [9] conducted a study of martensite treatment to low-carbon steel. They reported that the average ferrite size was 132 nm and the tensile strength was 978.1 MPa in a specimen with a reduction of 70% in thickness.

Despite much experimental research performed to explain the simple deformation of martensite, SPD of martensitic steel and subsequent annealing, remain unclear. In the present work, two martensites starting steel samples were severely deformed by the multi-directional forging and for a better investigation about the thermo-mechanical process, the texture evolution and mechanical properties were introduced.

Furthermore, to compare texture and mechanical properties, two other martensitic steel samples were deformed by plane strain compression (PSC). In both deformation methods, a total true strain of 2 and the same annealing procedure were applied.

2. Material and Methods

2.1. The Martensite Treatment

The material used in this study was commercial plain low-carbon steel whose chemical composition (in wt %) was Fe - 0.15% C - 0.64% Mn - 0.12% Si - 0.05% Cu - 0.015% S - 0.013% P. The initial samples for MDF were rectangular cubes with a height of 50 mm and a base of 40 \times 40 mm². The dimension of the plane strain compression samples was 50 (length) \times 10 (width) \times 4 (thickness) mm³. The sheets were austenitized at 1000 $^{\circ}\text{C}$ for 30 min in a laboratory furnace followed by iced brine quenching to produce the martensitic structure. The quenched specimens were selected and their surface was prepared with cleaning, wire brushing with a stainless steel brush and degreasing an acetone bath.

In the MDF method, forging was repeated up to 10 cycles. In-plane strain compression, forging was applied to 10 passes. The schematic of the MDF process for one cycle is presented in Figure 1. In

both techniques, the total true strain of 2 was applied. Finally, forged samples were annealed at two temperatures (450 °C and 550 °C) for 30 min.

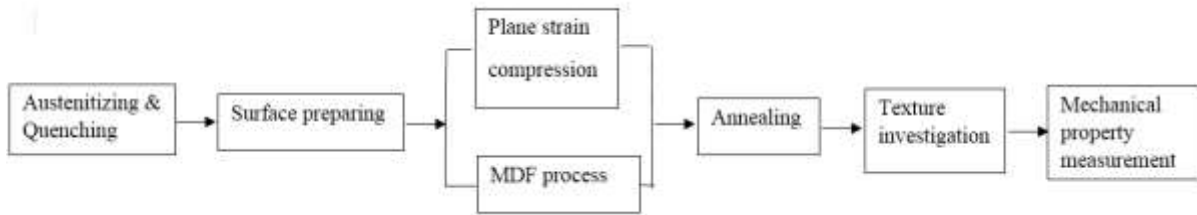


Figure1. Experimental system

2.2. Characterizations

The texture sample was prepared from the mid-section of the thickness of the sheets (longitudinal section) perpendicular to the TD cross-section. However, for this experiment, the specimens were mechanically polished in a solution containing 800 ml of acetic acid and 200 ml of HCl to prevent the residual stress from mechanical polishing remaining on the surface of the sheet. To measure the texture, X-ray diffraction method XRD (Philips X' Pert with Cu K α anode) and Philips X'Pert software were used. The pole figures of (111), (200), (220) and (311) were prepared.

The textures of the fabricated specimens are discussed using the orientation distribution function (ODF). The ODFs were calculated with the X'pert texture software. The Bunge notation, in which the crystal rotations are described by three Euler angles, ϕ_1 , ϕ , and ϕ_2 , is employed. Because most of the texture components in steel can be seen in the section of $\phi_2 = 45^\circ$, this section has been studied. The texture in this section is composed of two main orientation fibers: α -fiber ($\langle 110 \rangle$ parallel to RD of the sheet) and γ -fiber ($\langle 111 \rangle$ parallel to ND of the sheet) [10].

Micro-hardness testing was performed in the Vickers method at room temperature with a load of 300 g and a time duration of 10 seconds. Tensile tests were applied using a Santam tensile testing machine on samples prepared to conform to the JIS Z2201 standard, with a constant crosshead speed of 1 mm min⁻¹. The above experimental sequence is summarized as a block scheme in Figure 2.

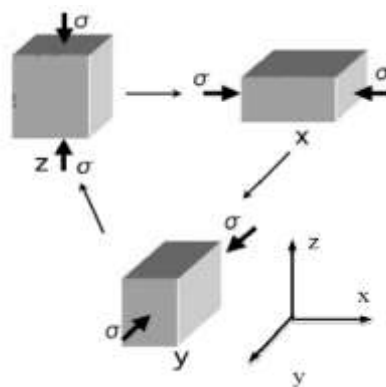


Figure2. One cycle of multi-directional forging (MDF) Schemes

3. Results

3.1 Texture evolution

Figure 3, shows the textures ($\varphi_2=45^\circ$ section of the ODFs) of plane strain compressed and MDFed specimens. In both forged specimens, a typical cold deformation texture is produced. This texture consists of two high-intensity α -fiber and γ -fiber. In both Figure 3a and b, a complete γ -fiber from $\{111\}\langle 110\rangle$ to $\{111\}\langle 112\rangle$ orientation and an incomplete fiber α (between $\{001\}\langle 110\rangle$ and $\{111\}\langle 110\rangle$ orientations) are observed.

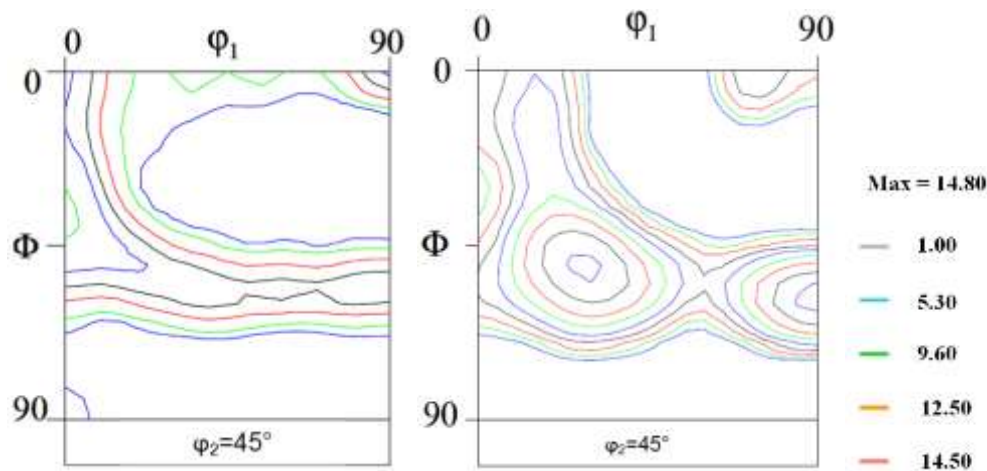


Figure 3. The $\varphi_2=45^\circ$ section of ODFs of investigated forged martensitic steel:
(a) By plane strain compression and (b) MDF method

For a better comparison of orientations in the two forged samples, α and γ skeleton lines are illustrated in Figure 4. In both samples, the overall shape of the α -fiber is very similar, and only the intensity of their orientations varies.

As shown in Figure 4a, in both samples, strong peaks near the $\{111\}\langle 110\rangle$ and $\{112\}\langle 110\rangle$ components of α -fiber occur. In-plane strain compressed sample, the intensity of $\{110\}\langle 110\rangle$ orientation is approximately 4 times the MDFed sample. In the γ -Fiber, in both specimens, the $\{111\}\langle 112\rangle$ and $\{111\}\langle 110\rangle$ orientations reach a maximum value. Of course, the intensity of these peaks is higher in the MDFed sample and the shape of the γ -fiber for plane strain compressed one is almost flat. After MDF, the intensity of $\{112\}\langle 110\rangle$ orientation in the α -fiber has increased from 7 to 11 times the normal.

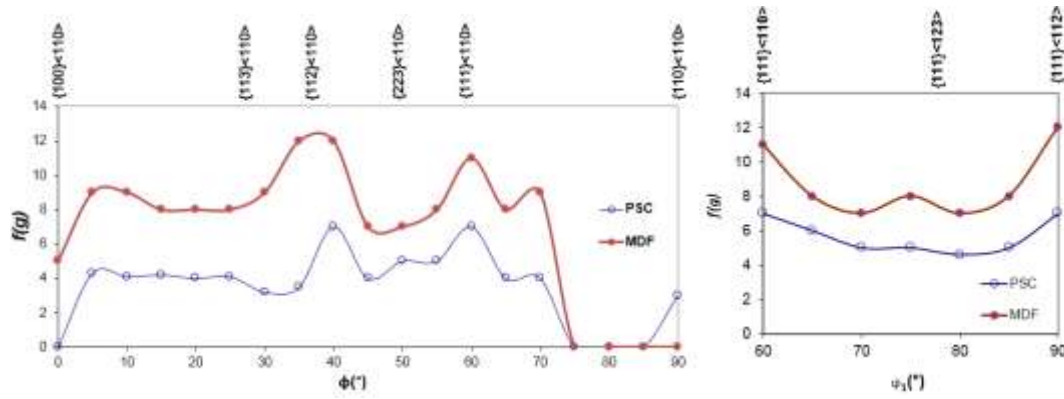


Figure4. Intensity distributions along α and γ -fiber texture of the plane strain compressed (PSC) and MDFed martensitic steel

In Figure 5, changes in component density for forged and tempered samples at 450 °C and 550 °C are given. In all ones, in Figures 5a - c, the γ -fiber is observed, but in Figure 5d, this fiber is faded. Instead, the α -fiber is only intense in Figure 5d, and in the rest of the samples, it almost disappears. In other words, in the MDFed specimen, after tempering at 550 °C, the γ -fiber has completely disappeared, and instead, the α -fiber and the rotated cube component have been reinforced (Figures 5b and d).

Figure 6, shows the intensity distributions along the α -fiber and γ -fiber determined from the ODFs of the forged and annealed samples. In Figure 6a, it is observed that by annealing at 450 °C, the intensity of the component $\{111\}\langle 110\rangle$ was reduced and added to the components $\{111\}\langle 123\rangle$ and $\{111\}\langle 112\rangle$.

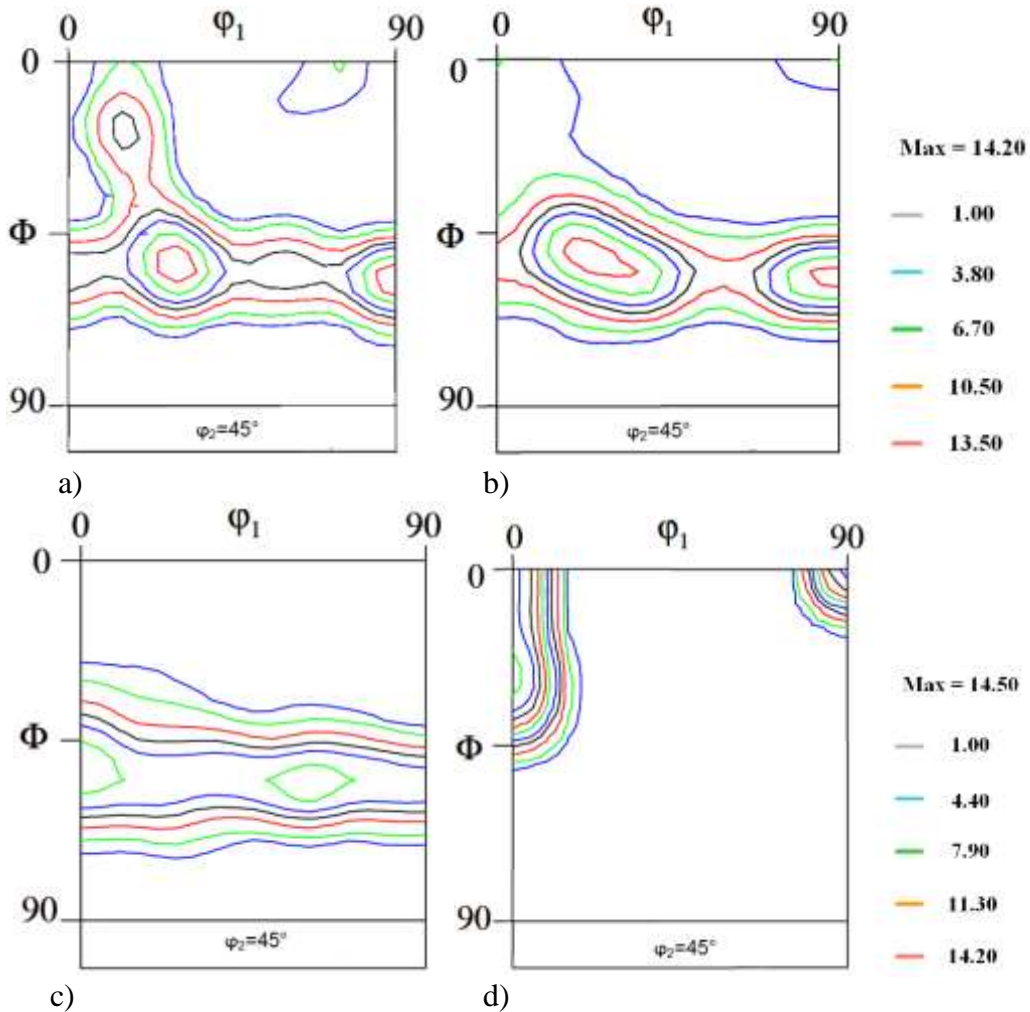


Figure 5. The $\varphi_2=45^\circ$ section of ODFs of annealed steels after a) plane strain compression and b) MDF at 450 °C for 30 min, c) Plane strain compression and d) MDF at 550 °C for 30 min

By comparing the intensity of the texture components in the two forged samples after annealing at 550 °C in Figure 6b, it can be concluded that the γ -fiber is more intense in the plane strain compressed one. Of course, compared to the as-forged mode (Figure 4), the intensity of the γ -fiber is reduced. But the named fiber has almost disappeared after MDF and annealing at this temperature. In the α -fiber, the intensity of the components of $\{110\}\langle 110\rangle$ and $\{111\}\langle 110\rangle$ was reduced to zero, but the intensity of the component $\{100\}\langle 110\rangle$ was roughly tripled, compared to the forged state (Figure 6).

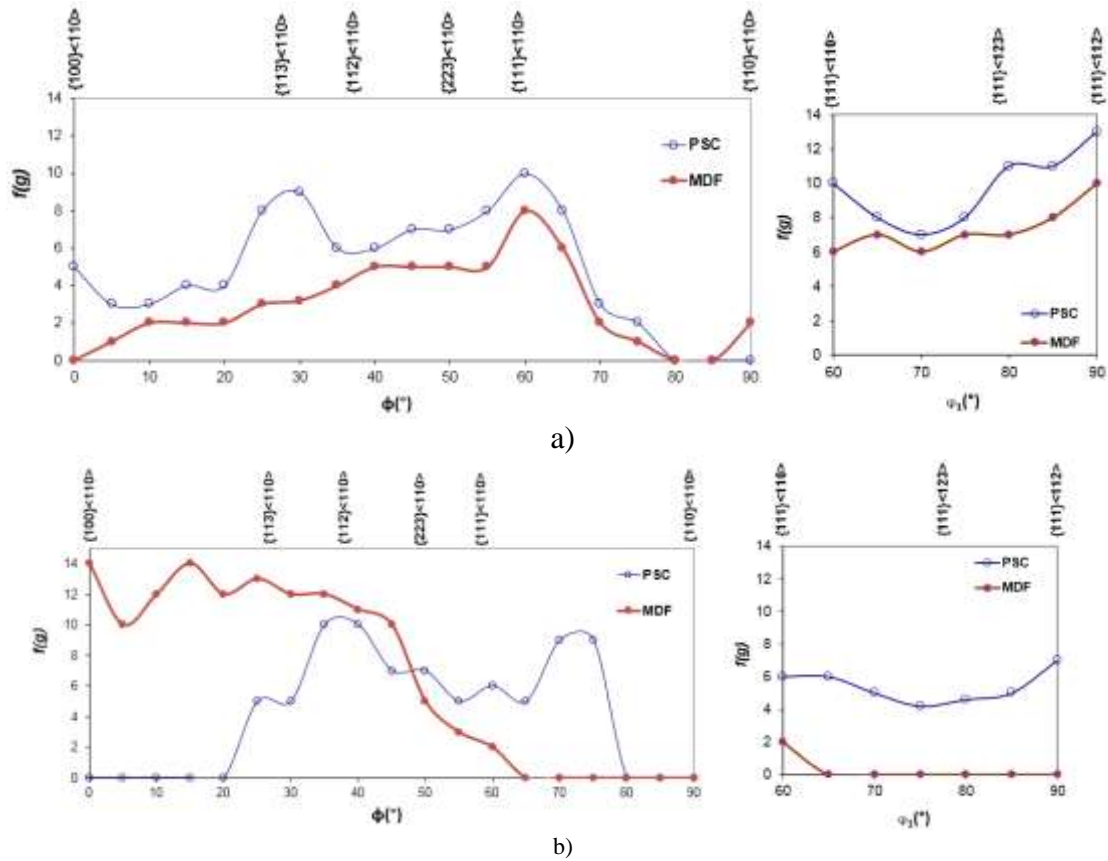


Figure6. Intensity distributions along α and γ -fibers of the plane strain compressed and MDF samples after annealing at (a) 450 °C and (b) 550 °C

3.2 Mechanical properties

Figure 7 shows the hardness, yield stress (YS) and ultimate tensile stress (UTS) in the received, quenched, deformed and annealed specimens. It can be seen that maximum hardness was observed MDFed specimen (382 HV), which was 2.4 higher than that of initial steel (Figure 7a).

According to the results, after MDF, the yield and ultimate strength greatly increased to 1278 and 1658 MPa, respectively. Therefore, the YS was approximately 4 times higher than that of the as-received steel, while it was 4.4 times higher for the UTS (Figure 7b). Generally, the hardness, YS, and UTS after PSC (conventional forging) are lower than MDFed martensite in the same strain level. Besides, after annealing of the MDFed specimens at 450°C for 30 min, the YS and UTS decreased to 748 and 1087 MPa, respectively. Thus, YS and UTS decreased with increasing annealing temperature. After annealing at 450 and 550°C for 30 min, YS and UTS in both PSC and MDFed samples decreased. But, the rate of strength decline in MDFed specimens was larger (Figure 7b and c).

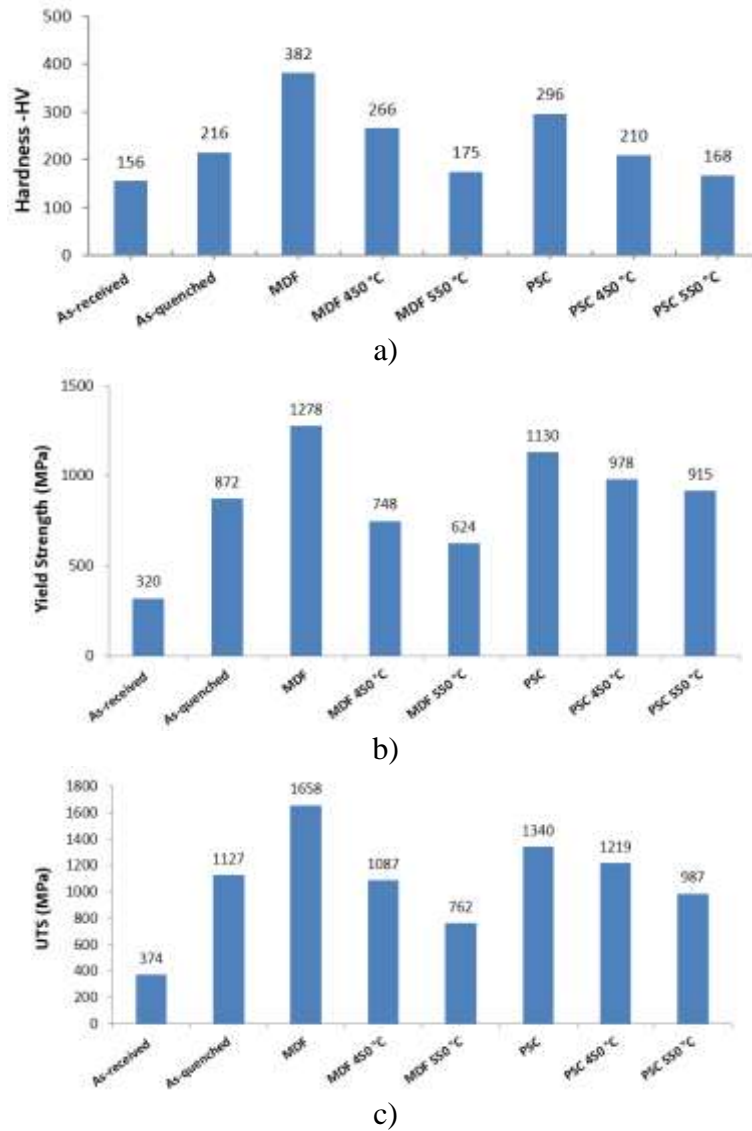


Figure 7. Hardness, YS, and UTS in as-received, as-quenched, deformed and annealed specimens for 30 min: a) Hardness (HV), b) YS (MPa) and c) UTS (MPa)

4. Discussion

4.1 Texture evolution

Formation of the deformation components in metals is the result of the slip and rotation of the crystalline network during deformation, and the easiest type of slip in the BCC metals occurs in the slip system $\{hkl\}\langle 111 \rangle$ [11]. In Figures 3 and 4, it can be seen that the dislocations slip in the plane $\{110\}$ and direction of $\langle 111 \rangle$, leads to strong $\{111\}$ grains and reinforcement of γ -fiber. In other words, the active slip systems in BCC crystalline structure also acts in the same way with ferrite steel with the BCC structure.

The shear texture components in steel are: $\{112\}\langle 110 \rangle$, $\{111\}\langle 110 \rangle$ and $\{111\}\langle 112 \rangle$ which in the ODF of both sheets in Figures 3 and 4 are also relatively enhanced. These components are formed in shear bands [12]. It can be concluded that in the forged martensitic structure, deformation

inhomogeneities, such as shear and transitional bands, are widely distributed. High shear stress, stored elastic strain, and dislocation network between the layers of the MDFed sample reinforce most of the shear texture components (Figure 4).

In the plane strain compressed sample, annealing results in complete removal of the α -fiber and the intensity of the γ -fiber (Figure 5a and c). The reason for this great difference in the evolution of the textual components during the annealing is due to the difference in their forging behavior. MDF leads to the formation of high inhomogeneity and shear stress in the structure that is contributed to the development of α -fiber and cubic components. Around some of the microstructural inhomogeneities, such as deformation, shear, and transitional bands, are suitable for nucleation and growth during recrystallization [13].

After annealing the plane strain compressed specimen at 450 °C, odd components appear at the section of $\varphi_2=45^\circ$ (Figure 5a). These components are fiber elements $\{h11\} \langle 1/h, 1, 2 \rangle$ that lie along the parallel line of the fiber α with angle φ between 0 and 35° [10]. The presence of α -fiber and the high intensity of the rotated cubic component before annealing is necessary to form this fiber during recrystallization, which in the named case this condition was present (Figure 4).

In other words, the γ -fiber changes occur within itself and the overall shape remains constant. Namely, new grains $\{111\}$ have been able to nucleate and grow with the use of the $\{111\}$ grains, and forging components of the γ -fiber have been disappeared and recrystallization components have been produced.

As a result of Figure 6a, grains $\langle 111 \rangle // ND$ have nucleated and grown predominantly due to more suitable substitutes. To grow recrystallized nuclei, their boundary angle must be high with the deformation components [14]. The γ -fiber is a combination of two types of forging and recrystallization components with a high angle between them, so during the annealing, their forging components are swallowed by annealing components.

The reason for the reduction of the components of γ -fiber in the plane strain compressed sample and disappearing of these components in the MDFed sample after annealing at 550 °C (Figure 6b), can be attributed to the stored energy of the grains. The nucleus with higher stored energy has higher growth potential at lower temperatures. The stored energy of the various grain orientations decreases as the order of $E \{110\} > E \{111\} > E \{112\} > E \{100\}$ [15].

Although the energy of the grains $\{110\}$ is the greatest, their number is usually very small in the forged structure. Grains $\{100\}$ are not usually consumed until the final stages of recrystallization. Grains $\{111\}$ have a higher degree of nucleation and growth [11]. These grains, tolerate the highest strain during MDF and thus have a high energy content, and as a result, have a high driving force for recrystallization.

On the other hand, the misorientation angle of the neighboring points in the strained grains of $\{001\} \langle 110 \rangle$ is very low and about 4°. While the misorientation value for MDFed grains of $\{111\} \langle 110 \rangle$, is high and 10° [11]. Due to the difference in the misorientation angle as well as the latent energy, the grains with the orientation of $\{111\} \langle 110 \rangle$ were consumed before the grains $\{100\} \langle 110 \rangle$ during annealing (Figure 5b). In Figure 5d, irregular growth in this sample is observed. The results showed that for each forging method, the mechanism of recrystallization and the development of texture is different. If in an example, the overall texture composition remains constant during recrystallization, the "oriented nucleation" mechanism is preferred, and in cases

where the recrystallization eliminates the particular strong component and other components appear, "selective growth" has been the dominant mechanism [16].

4.2 Mechanical properties

It is inferred from Figure 7 that higher strength of MDFed martensitic steel is attributed to the effect of severe plastic deformation which causes very fine and rotated martensite packets and high density of deformation in-homogeneities. Otherwise, reinforcement of the shear texture components in these specimens (Figure 4) results in strength improvement.

The decline of hardness with annealing temperature results from the martensite decomposition into ferrite and cementite, and grain coarsening. Larger rate of strength decline in MDFed specimens after annealing can be attributed to the existence of the higher stored energy. Thus, the rate of recrystallization and grain growth have been higher in these samples (Figure 7). This finding agrees with the reduction or disappearing of γ -fiber components in these samples after annealing at 450 and 550 °C (Figur 6).

5. Conclusion

In this study, to prove the effect of MDF on the final texture and mechanical properties, the PSC and MDFed martensitic steel were investigated in the same conditions. Main conclusions drawn were as follows:

- The active slip systems in the BCT crystalline structure of martensite acted so with ferrite steel with BCC structure. In previous researches, this issue has not been adequately addressed.
- In the PSCed specimens, since the components of α -fiber and γ -fiber were constant during recrystallization, the "oriented nucleation" theory was dominant during recrystallization.
- A basic change in the fibers during the annealing of the MDFed specimens indicated that it had precedence over the "selective growth".
- After MDF, the yield and ultimate strength of samples greatly increased to 1278 and 1658 MPa, respectively. Achieving these amounts of strength in low carbon steel has been challenging in related researches.
- The main reason for the higher rate of strength decline in MDFed samples after annealing was the presence of a higher density of dislocation and stored energy. This finding agrees with the reduction or disappearing of γ -fiber components in these samples after annealing.

6. References

- [1] Berecz, T. P., Jenei, A., Csore, J., Labar, J. and Gubicza, P. 2016. Determination of dislocation density by electron backscatter diffraction and X-ray line profile analysis in ferrous lath martensite. *Materials Characterization*. 113: 117-204.
- [2] Dastur, P., Zarei-Hanzaki, A., Pishbin M. H., Moallemi M. and Abedi H. R. 2017. Transformation and twinning induced plasticity in an advanced high Mn austenitic steel processed by martensite reversion treatment. *Materials Science and Engineering: A*. 696: 511-518.

- [3] El-Tahawy, M., Henrique P., Pereira R., Huang, Y., Park, H. and Gubicza, J. 2018. Exceptionally high strength and good ductility in an ultrafine-grained Aluminium and Brass. *Materials Letters*. 214: 240-245.
- [4] Ghosh, C., Haldar A. and Ghosh, P. 2008. Microstructure, Texture, Grain Boundary Characteristic. *ISIJ International*. 48: 1626-1631.
- [5] Hosseini, M., Kermanpur, A. and Najafizadeh, A. 2012. Effect of process parameters on microstructures and mechanical properties of a nano/ultrafine grained low carbon steel produced by martensite treatment using plane strain compression. *ISIJ International*. 52: 464-470.
- [6] Jafarian H. and Tarazkouhi, M. 2017. Significant enhancement of tensile properties through combination of severe plastic deformation and reverse transformation in an ultrafine/nano grain lath martensitic steel. *Materials Science and Engineering: A*. 686: 113119
- [7] Jafarian, H., Mousavi A., Eivani A. R. and Park N. 2017. A comprehensive study of microstructure development and its corresponding tensile properties in nano/ultrafine-grained metastable austenitic steel during accumulative roll bonding (ARB). *Materials Science and Engineering: A*. 703: 196-203.
- [8] Jiang, H., Liu, Y., Wu, Y., Zhao, K., Shan, D. and Zong, Y. 2019. Grain Refinement Mechanism and Microstructural Evolution of M50NiL Steel during Multi-directional Impact Forging', *Journal of Materials Engineering and Performance*, 12: 1-12.
- [9] Kalashami, A., Kermanpur, A., Najafizadeh, A. and Mazaheri, Y. 2017. The effect of Nb on texture evolutions of the ultrafine-grained dual-phase steels fabricated by cold rolling and intercritical annealing. *Journal of Alloys and Compounds*. 694: 1026-1033.
- [10] Kestens, L. and Pirgazi, H. 2016. Texture formation in metal alloys with cubic crystal structures. *Materials Science and Technology*. 32: 1303-1316.
- [11] Kishchik, M.S, Mikhaylovskaya, A.V., Kotov, D., Mosleh, A.O., AbuShanab, W.S. and Portnoy, V.K. 2018. Effect of multidirectional forging on the grain structure and mechanical properties of the Al–Mg–Mn alloy. *Materials*, 11(11): 2166-2178.
- [12] Markushev, M.V. 2011. On the methods of severe plastic deformation for bulk nano-materials processing. *Letters on Materials*, 1(1): 36-42.
- [13] Mikhaylovskaya, A.V., Kotov, D., Kishchik, M.S., Prosviryakov, A.S. and Portnoy, V.K. 2019. The effect of isothermal multi-directional forging on the grain structure, superplasticity, and mechanical properties of the conventional Al–Mg-based alloy. *Metals*. 9: 33-45.
- [14] Pereloma, E. and Edmonds, D. 2012. Phase transformations in steels, diffusionless transformations, high strength steels. modelling and advanced analytical techniques. Woodhead Publishing Limited.
- [15] Yuan, Q., Xu, G., Liu, S., Liu, M., Hu, H and Li, G. 2018. Effect of rolling reduction on microstructure and property of ultrafine grained low-carbon steel processed by cryorolling martensite. *Metals*. 8: 518-532.
- [16] Zheng, Z., Zhang, X., Xie, L., Huang, L. and Sun, T. 2019. Changes of microstructures and mechanical properties in commercially pure titanium after different cycles of proposed multi-directional Forging. *Metals*. 9:175-186.